Journal of Alloys and Compounds 507 (2010) 172–177

Contents lists available at ScienceDirect

Journal of Alloys and Compounds

journal homepage: www.elsevier.com/locate/jallcom

Synthesis, structural and electrochemical properties of $LiNi_{0.79}Co_{0.1}Mn_{0.1}Cr_{0.01}O_2$ via fast co-precipitation

Ling-jun Li, Xin-hai Li*, Zhi-xing Wang, Hua-jun Guo, Peng Yue, Wei Chen, Ling Wu

School of Metallurgical Science and Engineering, Central South University, Changsha 410083, PR China

ARTICLE INFO

Article history:
Received 12 July 2010
Received in revised form 18 July 2010
Accepted 20 July 2010
Available online 29 July 2010

Keywords:
Lithium ion battery
Cathode material
Cr substitution
Electrochemical behavior

ABSTRACT

A novel layered material of $LiNi_{0.79}Co_{0.1}Mn_{0.1}Cr_{0.01}O_2$ is synthesized by fast co-precipitation method. Transmission electron microscope (TEM) and energy dispersive analysis of X-rays (EDAX) exhibit that Cr is successfully incorporating into $LiNi_{0.8}Co_{0.1}Mn_{0.1}O_2$. X-ray diffraction (XRD) and Rietveld refinement show that cation mixing is reduced by Cr substitution. Cyclic voltammerty (CV) indicates that the Cr substitution could decrease Jahn–Teller distortion, and improve reversibility of Li^+ ions during intercalating/deintercalating. Electrochemical impedance spectroscopy (EIS) reveals that Cr substitution has an effect on restraining the charge transfer impedance of cathode. Electrochemical studies confirm that Cr substitution for $LiNi_{0.8}Co_{0.1}Mn_{0.1}O_2$ also results in improved discharge capacity, initial coulombic efficiency, rate ability and cycling property of cathode. The capacity retention of $LiNi_{0.8}Co_{0.1}Mn_{0.1}O_2$ after 50 cycles at 5C is only 76.1%, however, that of the $LiNi_{0.79}Co_{0.1}Mn_{0.1}Cr_{0.01}O_2$ is improved to 89.02%. It is noted that the discharge capacity of $LiNi_{0.79}Co_{0.1}Mn_{0.1}Cr_{0.01}O_2$ is 209.9, 183, 171.4, 164.2 and 152.8 mAh g^{-1} at 0.1, 1, 3, 5 and 10C, respectively, in the cut-off voltage of 2.7–4.3 V.

1. Introduction

Recently, layered $LiNi_{0.8}Co_{0.1}Mn_{0.1}O_2$ has been intensively studied as a potential positive active electrode for application in plug-in hybrid electric vehicles (P-HEVs) [1,2]. It is reported that this mixed oxide inherits the merits of mono metal oxide $LiCoO_2$, $LiNiO_2$ and $LiMnO_2$, and exhibits lower cost, less toxicity and higher capacity [3–6]. Nevertheless, there still remain many problems, such as low initial coulombic efficiency, poor rate capacity and poor cyclability due to cation mixing (some Ni^{2+} ions of Ni layer move to Li layer) and instable structure [7,8]. Many authors reported that partial transition metal substitution for Ni in $Li(Ni_{1-x}M_x)O_2$ (M = metal) can modify the structure and improve electrochemical properties [9–15]. Ohzuku et al. found that partial Al substitution for Ni effectively stabilizes the structure of $LiNiO_2$ system [9]. Woo et al. studied the impact of the Al and/or Mg substitutions on the $LiNi_{0.8}Co_{0.1}Mn_{0.1}O_2$ system and concluded that the improvement of electrochemical properties derives from the reduced cation mixing [10]. The substitution of Ni by a small amount of other cations such as Fe, Ga, Ti, Zn and Sr has also been found to improve cycling stability for the $Li(Ni_{1-x}M_x)O_2$ (M = metal) system [15–20]. However, reports about the effect of Cr substitution on $LiNi_{0.8}Co_{0.1}Mn_{0.1}O_2$ material are less common. In this study, we employed chromium (Cr^{3+}) as dopant, partly due to that Cr is an electrochemical active element, and partly due to that the Gibbs free energies of Cr_2O_3 (−1153.88 kJ/mol), and CrO_3 (−599.68 kJ/mol) are more negative than that of NiO (−211.7 kJ/mol) [21]. It is found that the order of the metal–oxygen bonding strength is $Cr^{+3/+6}$–O > Ni^{2+}–O, and assumed that the Cr substitution is conducive to $LiNi_{0.8}Co_{0.1}Mn_{0.1}O_2$.

To improve rate capability and cyclability of $LiNi_{0.8}Co_{0.1}Mn_{0.1}O_2$, small particles are also needed since they are easier for lithium insertion-extraction than larger particles [22,23]. However, it is difficult to prepare nanoparticles or submicron materials by traditional co-precipitation method, due to quite long reaction time (12 h) is usually needed to synthesize $Ni_{0.8}Co_{0.1}Mn_{0.1}(OH)_2$ precursor [1,10]. In this work, we prepare the hydroxide precursors in a very short time, only 1 min. Here, $LiNi_{0.8}Co_{0.1}Mn_{0.1}O_2$ and $LiNi_{0.79}Co_{0.1}Mn_{0.1}Cr_{0.01}O_2$ are successfully synthesized by our fast co-precipitation method, and the effects of Cr substitution on the structure and electrochemical properties of $LiNi_{0.8-x}Co_{0.1}Mn_{0.1}Cr_xO_2$ (x = 0, 0.01) materials are discussed in detail.

2. Experimental

2.1. Preparation of $LiNi_{0.8-x}Co_{0.1}Mn_{0.1}Cr_xO_2$ (x = 0, 0.01)

$Ni_{0.8-x}Co_{0.1}Mn_{0.1}Cr_x(OH)_2$ (x = 0, 0.01) precursors were synthesized by the following procedures: (1) $NiCl_2$ $6H_2O$, $CoCl_2$ $6H_2O$, $MnCl_2$ $4H_2O$ and $CrCl_3$ $6H_2O$ powders were dissolved in distilled water to obtain 2 mol/L solution. (2) The mixtures were heated at 50 °C in water bath kettle, then NH_3 H_2O (2 M) and NaOH (2 M)

* Corresponding author. Tel.: +86 731 88836633; fax: +86 731 88836633.
E-mail address: csullj@hotmail.com (X.-h. Li).

0925-8388/$ – see front matter © 2010 Elsevier B.V. All rights reserved.
doi:10.1016/j.jallcom.2010.07.148

Table 1
Results of the ICP analysis for $LiNi_{0.8-x}Co_{0.1}Mn_{0.1}Cr_xO_2$ ($x = 0, 0.01$) materials.

Sample	Molar ratio of the final product (±1%)				
	Li	Ni	Co	Mn	Cr
a	1.00	0.802	0.099	0.099	0.00
b	1.01	0.790	0.096	0.094	0.01

were quickly added into the solution to control the pH between 11 and 12 under Ar atmosphere. (3) After being stirred for 1 min, the solution was filtered. (4) The resulting precursors were washed with distilled water and dried at 80 °C.

Stoichiometric $LiOH{\cdot}H_2O$ was milled with the precursors for 0.5 h, and the obtained mixtures were sintered at 480 °C for 5 h, and then sintered at 750 °C for 15 h under O_2 atmosphere. After being cooled to room temperature, the $LiNi_{0.8-x}Co_{0.1}Mn_{0.1}Cr_xO_2$ (sample a: $x = 0$, sample b: $x = 0.01$) materials were obtained.

2.2. Sample characterization

Element amounts of $LiNi_{0.8-x}Co_{0.1}Mn_{0.1}Cr_xO_2$ materials were analyzed using inductively coupled plasma emission spectroscopy (ICP, IRIS intrepid XSP, Thermo Electron Corporation). The samples were analyzed by SEM (JEOL, JSM-5600LV), Transmission electron microscope (TEM) and energy dispersive analysis of X-rays (EDAX) by Tecnai G^2 20ST. The powder X-ray diffraction (XRD, Rint-2000, Rigaku) using CuKα radiation was employed to identify the crystalline phase of the synthesized material. X-ray Rietveld refinement was performed using FULLPROF program.

2.3. Electrochemical tests

The electrochemical properties of $LiNi_{0.8-x}Co_{0.1}Mn_{0.1}Cr_xO_2$ were measured by using 2025 button cell. Typical positive electrode loadings were in the range of 1.95–2 mg cm^{-2}, and an electrode diameter of 14 mm was used. The cathode was consisted of 80 wt.% active material, 10 wt.% acetylene black and 10 wt.% PVDF binder. A lithium metal foil was used as anode. $LiPF_6$ (1 M) in a 1:1:1 (v/v/v) mixture of dimethyl carbonate (DMC), Ethyl Methyl Carbonate (EMC) and ethylene carbonate (EC) was used as electrolyte. The assembly of the cells was carried out in Ar-filled glove box. Electrochemical tests were carried out using an automatic galvanostatic charge–discharge unit, NEWARE battery cycler, between 2.7 and 4.3 V versus Li/Li^+ electrode at room temperature. The cyclic voltamogram (CV) was operated at 0.1 mV s^{-1} between 2.7 and 4.5 V. The electrochemical impedance spectroscopy (EIS) measurements were conducted by a CHI660a impedance analyzer, using an amplitude voltage 5 mV and frequency range was 0.01–0.1 MHz.

3. Results and discussion

3.1. Morphology and X-ray diffraction

The ICP results of $LiNi_{0.8-x}Co_{0.1}Mn_{0.1}Cr_xO_2$ ($x = 0, 0.01$) materials are reported in Table 1. It is noted that the chemical composition for each element in $LiNi_{0.8-x}Co_{0.1}Mn_{0.1}Cr_xO_2$ is close to the stoichiometry. This demonstrates that our fast co-precipitation method is an effective way to synthesize well stoichiometrical compounds.

Fig. 1 presents the SEM images for $LiNi_{0.8-x}Co_{0.1}Mn_{0.1}Cr_xO_2$ ($x = 0$, 0.01) materials. As shown, the particle morphologies of images are near-spherical and well distributed, and the average particle size is about 100–400 nm. Fig. 2 shows the TEM of sample b and its corresponding EDAX analysis, which is carried out at the edge and inside of the $LiNi_{0.79}Co_{0.1}Mn_{0.1}Cr_{0.01}O_2$ particle, and named points 1 and 2, respectively. It can be clearly seen that the spectra of Cr appears, and no great difference of elements contents is observed between the points 1 and 2. The result suggests that Cr is successfully incorporating into $LiNi_{0.8}Co_{0.1}Mn_{0.1}O_2$, and the distribution of all elements is homogenous.

The XRD patterns for the $LiNi_{0.8-x}Co_{0.1}Mn_{0.1}Cr_xO_2$ ($x = 0$, 0.01) materials and corresponding Rietveld refinement results are presented in Fig. 3 and Table 2, respectively. All the diffraction lines are indexed on the basis of the rhombohedral α-$NaFeO_2$ structure with a space group of R-3m. There is no impurity phase detected in the patterns, which indicates that a single phase layered $LiNi_{0.8-x}Co_{0.1}Mn_{0.1}Cr_xO_2$ is obtained. In this work, we performed the refinements assuming several scenarios: full and partial occupation of Cr in the Li and/or Ni layers. As seen in Fig. 3 and Table 2, the full occupation of Cr in the Ni layer resulted in good agreement between the observed and calculated patterns, with high reliability factors, and the cell volumes of sample b is smaller than that of sample a. This is because the ionic radius of Cr^{3+} (0.62 Å) is very close to that of Ni^{2+} (0.69 Å) [24], so that occupation of Cr in the Ni layer is highly possible. Additionally, the c/a ratio of sample b (4.945) is larger than that of undoped one (4.9435), indicating the Cr substituted sample has the higher layer properties [25,26]. The Ni/Li cation mixing amount of samples a and b is 2.5% and 6.8%, respectively, which means that Cr substitution for Ni could decrease cation mixing. The decreased cell volume, suppressed cation mixing, and increased c/a ratio could consequently induce the improvement of its initial coulombic efficiency, rate capacity and cycling ability.

3.2. Electrochemical behavior

The initial charge–discharge curves of $LiNi_{0.8-x}Co_{0.1}Mn_{0.1}Cr_xO_2$ ($x = 0$, 0.01) powders are shown in Fig. 4. The cells were measured at room temperature, between the voltage limits of 2.7–4.3 V and at 0.1C rate (18 mA g^{-1}), respectively. The initial charged and discharge capacity, and the corresponding coulombic efficiency of sample a is about 254.9, 192.42 mAh g^{-1}, and 75.5%, respectively. Great differences in the capacity and coulombic efficiency are observed in the sample b, which is about 238.08, 209.92 mAh g^{-1}, and 88.2%, respectively. It is noted that the initial charge capacity decreases, and the initial discharge capacity and coulombic efficiency improve after Cr substitution; the results are consistent

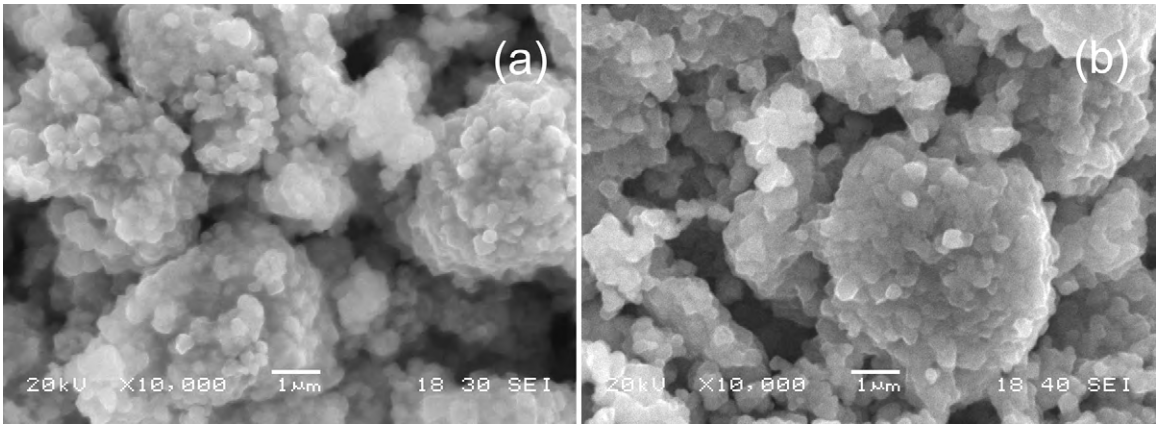

Fig. 1. SEM of $LiNi_{0.8-x}Co_{0.1}Mn_{0.1}Cr_xO_2$ powders: (a) $x = 0$ and (b) $x = 0.01$.

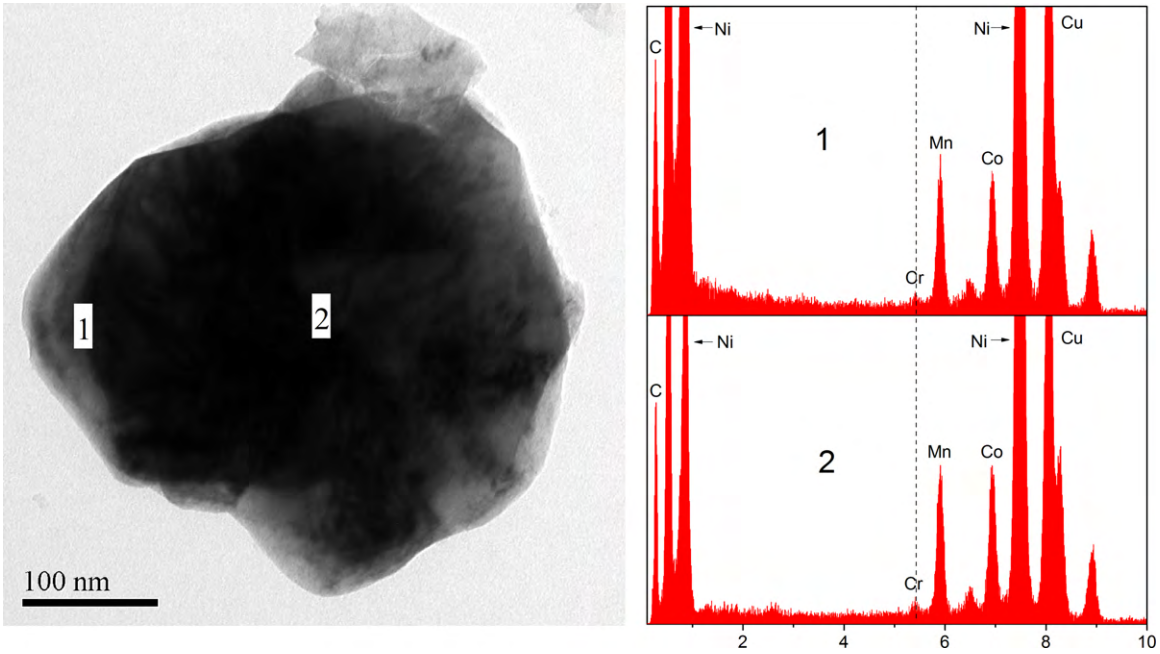

Fig. 2. TEM of $LiNi_{0.79}Co_{0.1}Mn_{0.1}Cr_{0.01}O_2$ particle and its corresponding EDAX spectra.

with Li's study [27]. One of the reasons is that Cr substitution could increase the amount of electrochemical active component in doped materials. The other is related to the suppressed cation mixing caused by Cr substitution (see XRD data). Delmas et al. [15] ascribed the initial irreversible loss of capacity to the oxidation of pre-existing Ni^{2+} ions which occupy the Li layer. Thus, less cation mixing in the Li layer for $LiNi_{0.79}Co_{0.1}Mn_{0.1}Cr_{0.01}O_2$ material, and additional electrochemical active component, caused by Cr substitution, result in more discharge capacity and coulombic efficiency.

Fig. 5 shows the rate capabilities of $LiNi_{0.8-x}Co_{0.1}Mn_{0.1}Cr_xO_2$ (a) $x = 0$, and (b) $x = 0.01$. The cells were charged to 4.3 V at 0.1, 1, 3 and 5C, and then discharged to 2.7 V at 1, 3, 5 and 10C, respectively. It is found that the discharge capacity of all samples decreases due to polarization as the current density increases. The initial discharge capacity of sample a is 148.9, 131.3, 123.1 and 103.7 mAh g^{-1} at 1, 3, 5 and 10C. However, the rate capability is improved significantly by Cr substitution. The sample b presented a capacity of 183, 171.4, 164.2 and 152.8 mAh g^{-1} at 1, 3, 5 and 10C. The better rate capability of sample b could also be ascribed to the additional electrochemical active component and less cation mixing in the Li layer for $LiNi_{0.79}Co_{0.1}Mn_{0.1}Cr_{0.01}O_2$ material.

The charge–discharge capacity versus cycle number for the $LiNi_{0.8-x}Co_{0.1}Mn_{0.1}Cr_xO_2$ (a) $x = 0$, and (b) $x = 0.01$ cells are given in Fig. 6. The cells were initially charged at 3C, and then discharged and charged at 5C in the range of 2.7–4.3 V for 50 times. The wavy curves should be ascribed to room temperature change. It is obvious that the sample a suffered a severe capacity fading and reaches to 93.6 mAh g^{-1} after 50 cycles. The capacity retention is only 76.1% of its initial discharge capacity. The sample b, attained its initial discharge capacity of 164 mAh g^{-1}, and reached 146 mAh g^{-1} after 50 cycles. It is noted that the capacity retention of sample b is improved to 89.02%. The improvement of capacity retention of layered materials is possible due to that the bonding energy of Cr-O is much stronger than that of Ni–O, therefore, Cr substitution could result in more stable structure; and partly due to some structural changes, the result could be proved by the following CV tests.

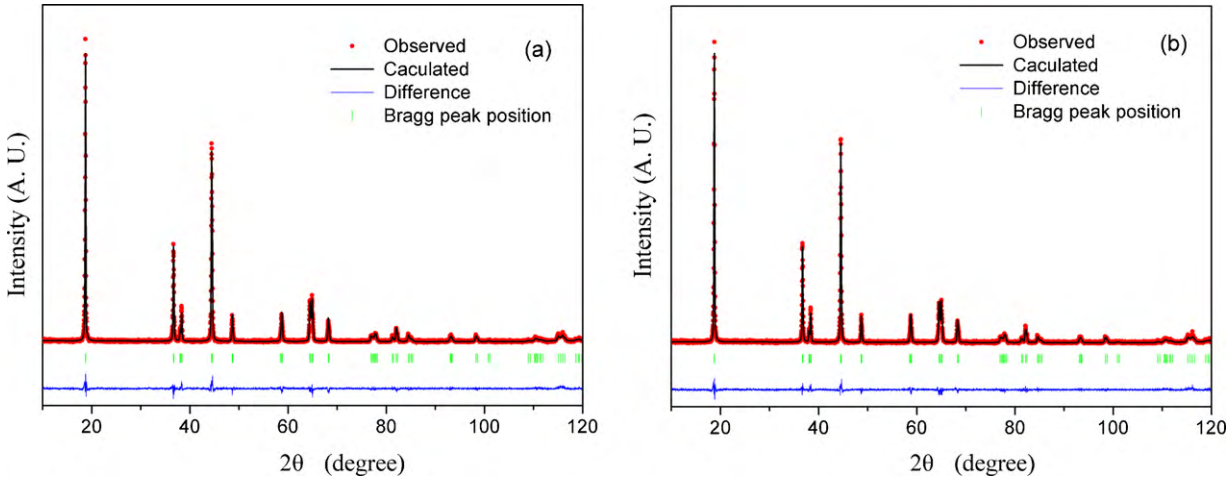

Fig. 3. Rietveld refinement results of X-ray diffraction patterns of $LiNi_{0.8-x}Co_{0.1}Mn_{0.1}Cr_xO_2$: (a) $x = 0$ and (b) $x = 0.01$.

Table 2
Structural parameters obtained from Rietveld refinement of the XRD data for $LiNi_{0.8-x}Co_{0.1}Mn_{0.1}Cr_xO_2$ ($x = 0, 0.01$).

Formula $a = b = 2.87195\ (4)$ Å, $c = 14.19751\ (5)$ Å, Rp = 7.4, Rwp = 10.6, Rexp = 4.51					$LiNi_{0.802}Co_{0.099}Mn_{0.099}O_2$ $V = 117.10$ Å^3, $c/a = 4.9435$	
Atom	Site	x	y	z	Occupancy	B (Å^2)
Li_1	3b	0	0	1/2	0.932 (4)	0.81 (5)
Ni_2	3b	0	0	1/2	0.068 (4)	0.81 (5)
Ni_1	3a	0	0	0	0.802 (5)	1.24 (9)
Co_1	3a	0	0	0	0.099	1.24 (9)
Mn_1	3a	0	0	0	0.099	1.24 (9)
O	6c	0	0	0.259 (11)	2.000	0.8
Formula $a = b = 2.86878\ (4)$ Å, c = 14.18604 (5) Å, Rp = 7.09, Rwp = 8.8, Rexp = 1.85					$LiNi_{0.799}Co_{0.096}Mn_{0.094}Cr_{0.01}O_2$ $V = 116.75$ Å^3, $c/a = 4.945$	
Atom	Site	x	y	z	Occupancy	B (Å^2)
Li_1	3b	0	0	1/2	0.975 (2)	0.62 (4)
Ni_2	3b	0	0	1/2	0.025 (2)	0.62 (4)
Ni_1	3a	0	0	0	0.799 (3)	1.07 (8)
Co_1	3a	0	0	0	0.096	1.07 (8)
Mn_1	3a	0	0	0	0.094	1.07 (8)
Cr_1	3a	0	0	0	0.011 (3)	1.07 (8)
O	6c	0	0	0.2591 (9)	2.000	0.8

$[n(Li_1) + n(Ni_2) = 1,\ n(Ni_1) + n(Co_1) + n(Mn_1) + n(Cr_1) = 1]$.

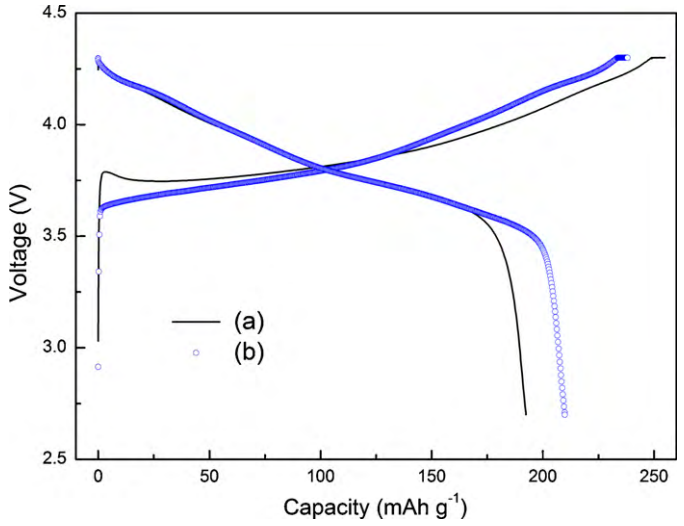

Fig. 4. Initial charge–discharge curves of $LiNi_{0.8-x}Co_{0.1}Mn_{0.1}Cr_xO_2$ coin cells (a) $x = 0$ and (b) $x = 0.01$. Experiments were carried out at constant current 0.1C rate (18 mA g^{-1}) in a range of 2.7 and 4.3 V.

3.3. Cyclic voltammetry (CV)

Cyclic voltammetry (CV) is a useful electrochemical tool wherein the changes taking place in an electrochemical reaction is monitored by measuring the current-potential responses. Fig. 7 compares the CV profiles of $LiNi_{0.8-x}Co_{0.1}Mn_{0.1}Cr_xO_2$ cells. It is noted that no cathodic peak near 3 V region in both samples, this indicates there is no reduction of Mn^{3+}/Mn^{4+}, according to Paulsen et al. [28]. It is also found that the difference of the curves on the first and second cycle is decreased significantly by Cr substitution. Furthermore, for $LiNi_{0.79}Co_{0.1}Mn_{0.1}Cr_{0.01}O_2$, a distinct decrease of the cathodic peak area near 4.0 V (indicated with arrow) was observed, the cathodic peak is probably identified as Ni^{4+}/Ni^{3+} process. It is reported that the irreversible layered spinel transition is related to the Ni^{4+}/Ni^{3+} process [29], suggesting the undesired Jahn–Teller distortion ($Ni^{4+} \rightarrow Ni^{3+}$ reduction reaction) has been suppressed by Cr substitution. These results are well consistent with the cycling performance of the studied material, meaning the reversible capacity and structure stability of $LiNi_{0.79}Co_{0.1}Mn_{0.1}Cr_{0.01}O_2$ compound are greatly improved.

It is noted that the anodic peak for the sample a in the first cycle centers at 3.90 and 4.22 V, respectively, another weak peak cannot

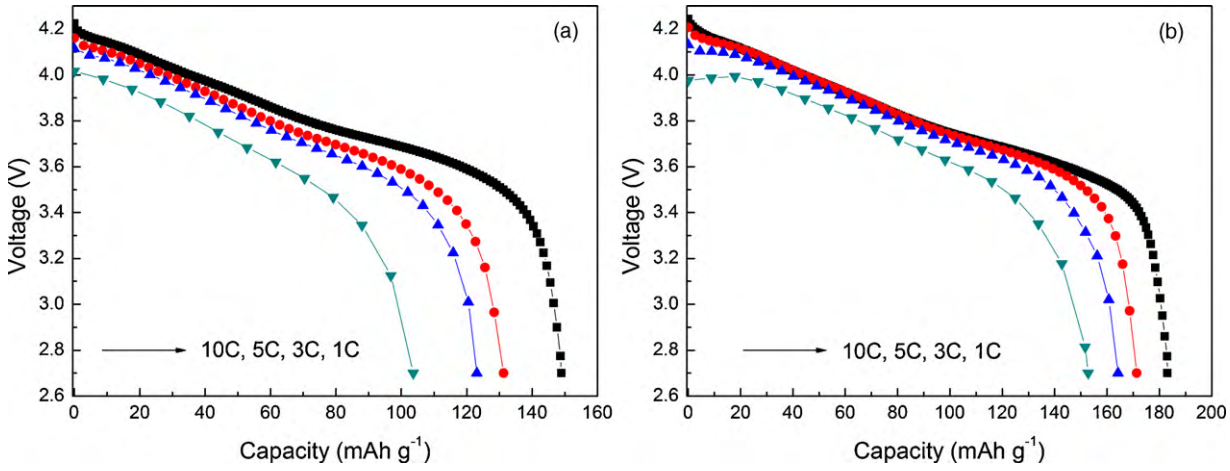

Fig. 5. Initial discharge curves of $LiNi_{0.8-x}Co_{0.1}Mn_{0.1}Cr_xO_2$ coin cells (a) $x = 0$ and (b) $x = 0.01$. Experiments were carried out at different current densities in a range of 2.7 and 4.3 V.

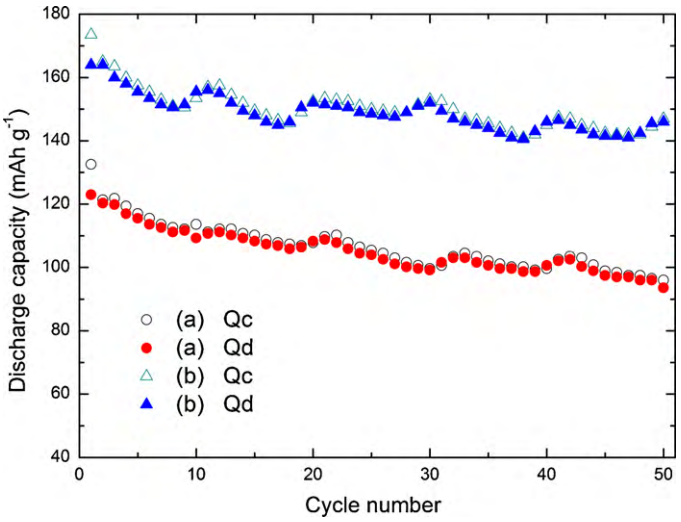

Fig. 6. Charge–discharge capacities of $LiNi_{0.8-x}Co_{0.1}Mn_{0.1}Cr_xO_2$ cells (a) $x = 0$ and (b) $x = 0.01$. Experiments were cycled 50 times at a 5C rate (900 mA g^{-1}) in a range of 2.7 and 4.3 V.

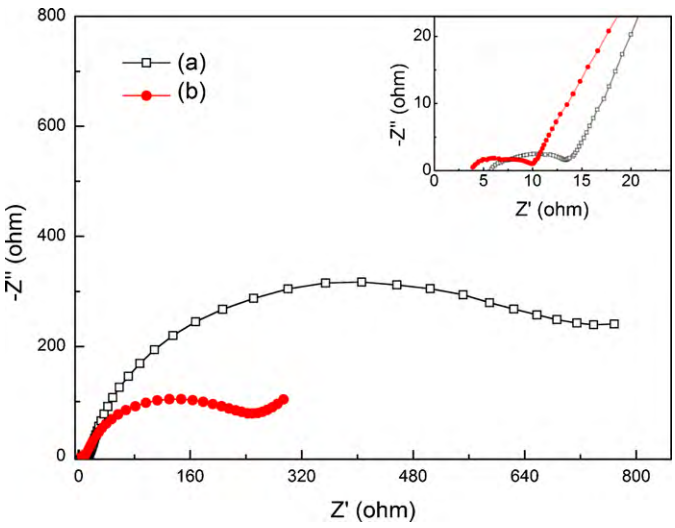

Fig. 8. Impedance spectra of $LiNi_{0.8-x}Co_{0.1}Mn_{0.1}Cr_xO_2$ cells: (a) $x = 0$ and (b) $x = 0.01$. Detailed EIS data in the 0–24 range is shown as an inset.

be very clearly discerned in the CV curves. And the corresponding cathodic peaks shift to 3.71, 4.14 and 3.96 V, respectively. For the sample b, the anodic peaks center at 3.83, 4.03 and 4.21 V, and the cathodic peaks at 3.71, 3.97 and 4.15 V. This implies that Cr substitution suppressed the potential difference of the major peak, from 0.19 V (sample a) to 0.12 V (sample b). This also indicates the better reversibility of Li^+ ions during intercalating/deintercalating in $LiNi_{0.79}Co_{0.1}Mn_{0.1}Cr_{0.01}O_2$ compound. Therefore, it could be concluded that Cr substitution improves structural stability and electrochemical properties of $LiNi_{0.8}Co_{0.1}Mn_{0.1}O_2$.

3.4. Electrochemical impedance spectroscopy (EIS)

Fig. 8 shows the EIS profiles of $LiNi_{0.8-x}Co_{0.1}Mn_{0.1}Cr_xO_2$ cells after 50 cycles at 5C, detailed EIS data in the 0–24 range is shown as an inset. Both spectra have the high-frequency semicircles, intermediate-frequency semicircles and low-frequency tails, which relate the surface-film resistance (R_{sei}), charge-transfer resistance (R_{ct}), and Warburg impedance [30], respectively. The value of R_{sei} and R_{ct} for sample a is 7.7 and 734.5 Ω (calculated from the semicircle's diameter), respectively. For the sample b, the R_{sei} and R_{ct} is 6.1 and 243.7 Ω. It is noted that the R_{sei} of sample a is similar to that of sample b. However, the R_{ct} of sample a is significantly larger than that of sample b. These results indicate that Cr substitution has an positive effect on restraining the charge transfer impedance of cathode. Small impedance is conducive to the intercalating/deintercalating of Li^+ ion. Therefore, the electrochemical properties of $LiNi_{0.8}Co_{0.1}Mn_{0.1}O_2$ can be greatly improved by Cr substitution.

4. Conclusion

Single phase $LiNi_{0.79}Co_{0.1}Mn_{0.1}Cr_{0.01}O_2$ was successfully synthesized by fast co-precipitation method. The morphological and EDAX characterization show that $LiNi_{0.79}Co_{0.1}Mn_{0.1}Cr_{0.01}O_2$ has 100–400 nm particle size and very well elements distribution. Electrochemical tests show that the Cr substitution sample exhibits improved discharge capacity, initial coulombic efficiency, rate ability and cycling property, compared to that of pristine sample. Rietveld refinements, CV and EIS results confirm that these improvements are attributed to less cation mixing, suppressed Jahn–Teller distortion, additional electrochemical active component and better reversibility of Li^+ ions during intercalating/deintercalating, caused by Cr substitution.

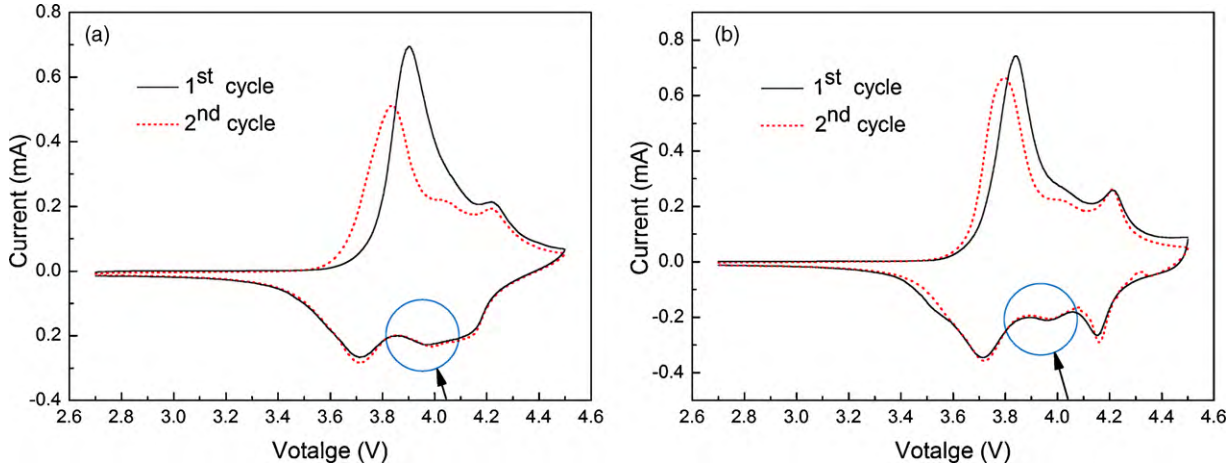

Fig. 7. Cyclic voltammogram of $LiNi_{0.8-x}Co_{0.1}Mn_{0.1}Cr_xO_2$ cells at a scan rate of 0.1 mV s^{-1}: (a) $x = 0$ and (b) $x = 0.01$.

Acknowledgement

This work was financially sponsored by the National Basic Research Program of China (973 Program, Contract No. 2007CB613607).

References

[1] M.-H. Kim, H.-S. Shin, D. Shin, Y.-K. Sun, J. Power Sources 159 (2006) 1328–1333.
[2] Y.K. Sun, S.T. Myung, B.C. Park, J. Prakash, I. Belharouak, K. Amine, Nat. Mater. 8 (2009) 320–324.
[3] J. Eom, M.G. Kim, J. Cho, J. Electrochem. Soc. 155 (2008) A239–A245.
[4] J.J. Saavedra-Arias, N.K. Karan, D.K. Pradhan, A. Kumar, S. Nieto, R. Thomas, R.S. Katiyar, J. Power Sources 183 (2008) 761–765.
[5] L. Croguennec, Y. Shao-Horn, A. Gloter, C. Colliex, M. Guilmard, F. Fauth, C. Delmas, Chem. Mater. 21 (2009) 1051–1059.
[6] Y.X. Gu, F.F. Jian, J. Phys. Chem. C 112 (2008) 20176–20180.
[7] J. Cho, T.J. Kim, J. Kim, M. Noh, B. Park, J. Electrochem. Soc. 151 (2004) A1899–A1904.
[8] Y.K. Sun, S.T. Myung, M.H. Kim, J.H. Kim, Electrochem. Solid State Lett. 9 (2006) A171–A174.
[9] T. Ohzuku, A. Ueda, M. Kouguchi, J. Electrochem. Soc. 142 (1995) 4033–4039.
[10] S.W. Woo, S.T. Myung, H. Bang, D.W. Kim, Y.K. Sun, Electrochim. Acta 54 (2009) 3851–3856.
[11] J.F. Xiang, C.X. Chang, F. Zhang, J.T. Sun, J. Electrochem. Soc. 155 (2008) A520–A525.
[12] F. Wu, M. Wang, Y. Su, L. Bao, S. Chen, J. Power Sources 195 (2010) 2900–2904.
[13] H.B. Kim, B.C. Park, S.T. Myung, K. Amine, J. Prakash, Y.K. Sun, J. Power Sources 179 (2008) 347–350.
[14] J. Cho, Chem. Mater. 12 (2000) 3089–3094.
[15] C. Delmas, M. Menetrier, L. Croguennec, I. Saadoune, A. Rougier, C. Pouillerie, G. Prado, M. Grune, L. Fournes, Electrochim. Acta 45 (1999) 243–253.
[16] Y. Nishida, K. Nakane, T. Satoh, J. Power Sources 68 (1997) 561–564.
[17] H. Liu, J. Li, Z. Zhang, Z. Gong, Y. Yang, Electrochim. Acta 49 (2004) 1151–1159.
[18] G.T.K. Fey, J.G. Chen, V. Subramanian, T. Osaka, J. Power Sources 112 (2002) 384–394.
[19] G.T.-K. Fey, V. Subramanian, J.-G. Chen, Mater. Lett. 52 (2002) 197–202.
[20] Y.H. Ding, P. Zhang, D.S. Gao, J. Alloy Compd. 456 (2008) 344–347.
[21] W. Li, J.N. Reimers, J.R. Dahn, Solid State Ionics 67 (1993) 123–130.
[22] A.C. Dillon, A.H. Mahan, R. Deshpande, P.A. Parilla, K.M. Jones, S.H. Lee, Thin Solid Films 516 (2008) 794–797.
[23] P.L. Taberna, S. Mitra, P. Poizot, P. Simon, J.M. Tarascon, Nat. Mater. 5 (2006) 567–573.
[24] R. Shannon, Acta Crystallogr. A 32 (1976) 751–767.
[25] S.W. Oh, S.H. Park, C.-W. Park, Y.-K. Sun, Solid State Ionics 171 (2004) 167–172.
[26] Y.M. Choi, S.I. Pyun, S.I. Moon, Solid State Ionics 89 (1996) 43–52.
[27] L.F. Jiao, M. Zhang, H.T. Yuan, M. Zhao, H. Guo, W. Wang, X. Di Zhou, Y.M. Wang, J. Power Sources 167 (2007) 178–184.
[28] J.M. Paulsen, C.L. Thomas, J.R. Dahn, J. Electrochem. Soc. 147 (2000) 861–868.
[29] M.G.S.R. Thomas, W.I.F. David, J.B. Goodenough, P. Groves, Mater. Res. Bull. 20 (1985) 1137–1146.
[30] M.D. Levi, K. Gamolsky, D. Aurbach, U. Heider, R. Oesten, Electrochim. Acta 45 (2000) 1781–1789.